Journal of Advances in Science and Technology
Vol. 16, Issue No. 1, March-2019, ISSN 2230-9659

Analysis of the Optical Properties of Functionalized Gold Nanoparticles in Different Tissues and Their Association with the Rise in Temperature

Komal[1]* Dr. Vipin Kumar[2]

[1] PhD Scholar, OPJS University, Churu, Rajasthan

[2] Associate Professor, OPJS University, Churu, Rajasthan

Abstract – Mie theory describes the association of light through the absorption (Cabs), scattering (Csca), and extinction (Cext) cross-sections with a gold nanoparticle (AuNP) such parameters were determined for AuNPs distributed in homogeneous media, but not for particular tissues. The goal of this research was to obtain theoretically, through Mie theory, the optical cross sections (Cabs, Csca, and Cext) of functionalized AuNPs in liver and colon tissues and compare them with the temperature increase observed experimentally in tissues containing AuNPs under plasmonic photothermal irradiation using a laser Nd-YAG (α = 532 nm). Calculations have shown that Cabs account for 98.96 ± 0.03 percent of Cext at 532 nm. The Cext value for a practical AuNP in water was 365,66 nm2 (94 percent of the maximum theoretical value at 522,5 nm), 404,24 nm2 in colon (98 percent of the maximum theoretical value at 525 nm), and 442,39 nm2 in liver (96 percent of the maximum theoretical value at 525 nm). Nanoparticles irradiated at 532 nm therefore come very close to their resonance value. Such findings were consistent with the experimental irradiation of functionalized AuNPs in different tissues, where the average rise in temperature showed liver pattern > colon > water. The observed increase in temperature (available up to 13∘C) is necessary to produce cell demise.

----------X----------

1. INTRODUCTION

The optical properties (assimilation and dissipating) present in gold nanoparticles (AuNPs) assume a critical job in the improvement of new photothermal removal frameworks possibly relevant in malignant growth treatment [1–3]. The photothermal removal process produced by AuNPs is because of the optical retention wonder present when AuNPs are presented to light that instigates an aggregate wavering of the free electrons (surface plasmon reverberation, SPR) [1, 4–6]. The temperature around the AuNPs arrives at 800∘ C and makes irreversible warm pulverization the tissue [7–11]. Gold nanoparticles (AuNPs) have been orchestrated in different sizes and shapes, for example, circles, poles, cubic, and crystals structures [12, 13]. A portion of these structures have been proposed for an assortment of clinical applications [2, 3, 14, 15]. Numerous biomolecules, for example, DNA chains, proteins, peptides, and aptamers can be conjugated to one AuNP [3]. The ArgGly-Asp (RGD) grouping has been accounted for to have high partiality and selectivity for the $\alpha(v)\beta(3)$ integrin.

This integrin is communicated on the outside of sound endothelial cells at low levels yet is overexpressed in the tumor neovasculature of osteosarcoma, neuroblastoma, glioblastoma, melanoma, lung carcinoma, and bosom cancer.The SPR band power and frequency attributes of the AuNPs rely upon factors influencing the electron charge thickness on the molecule surface, for example, the metal sort, molecule size, shape, structure, creation, and the dielectric consistent of the encompassing medium (water, kind of tissue). In the SPR marvel, the electrons of gold reverberate because of approaching radiation, causing both the assimilation and dispersing of light; these procedures can be clarified by Mie hypothesis. This methodology gives precise diagnostic answers for Maxwell's conditions for circles with different distances across; the ingestion and dispersing probabilities are spoken to by the retention, dissipating, and annihilation cross segments(C_{abs}, C_{sca}, and C_{ext}).

The optical retention and dispersing wonders firmly rely upon the size of the nanoparticles and the dielectric steady of the encompassing medium. For little AuNPs in water (refractive file n = 1.33 and

dielectric steady $\varepsilon=n^2$), all out annihilation is totally managed by retention; when the size builds, the dissipating procedure shows up and intensifies.

The hypothetical counts of the C_{abs}, C_{sca}, and C_{ext} coefficients through Mie hypothesis have been recently announced on account of light connecting with AuNPs scattered in a homogeneous medium, where the refractive list is viewed as a consistent. Be that as it may, such boundaries have not been resolved for explicit tissues, where the refractive file must be assessed as an element of the cooperating frequency since the retention and dissipating cross segments are firmly influenced by the structure of the tissue (measure of the water, hemoglobin, and melanin).

The assurance of these boundaries could clarify the temperature increment produced by the AuNP, which is a basic point in the expected clinical use of the plasmonic photothermal treatment. This examination expected to figure the optical coefficients (C_{abs}, C_{sca}, and C_{ext}) of functionalized gold nanoparticles in various tissues (liver and colon) by Mie hypothesis and to decide their relationship with the temperature increment watched tentatively in tissues containing AuNPs under plasmonic photothermal light utilizing a Nd-YAG lase

2. MATERIALS AND METHODS

2.1. Materials.

Gold nanoparticles (20 nm) were acquired from Sigma-Aldrich (6.54 × 1011 particles/mL). A 50 μM arrangement of c [RGDfK(C)] and PBS pH 7 was set up in type I grade water. Homogeneous suspensions of pork liver and chicken intestinal viscera (for recreating colon tissue) were mixed with a little volume of water. The blends were then gone through a sifter for sieving and homogenization.

2.2. Readiness of the AuNP-c[RGDfK(C)] Conjugate.

The union of cyclo[Arg-Gly-Asp-Phe-Lys(Cys)] (c[RGDfK(C)]) was done by the technique announced by FerroFlores et al. [14]. In the c[RGDfK(C)] atom, the succession Arg-Gly-Asp-(-RGD-) goes about as the dynamic natural site. The D-Phe (f) and Lys (K) buildups finished the cyclic and the pentapeptide structure, and Cys (C) is the spacer that contains the dynamic thiol bunch that connects with the gold nanoparticle surface. For conjugate planning, a 50 μM arrangement of c[RGDfK(C)] was readied utilizing type I grade water, and afterward 0.02 mL (6.023 × 1014 atoms) was added to 1 mL of the AuNP suspension (20 nm, 6.54 × 1011 particles/mL) trailed by blending for 5 min. No further cleansing was required.

2.3. Portrayal when Laser Illumination.

Prior to laser light, the synthetic conjugation was affirmed by UV-Vis, medium-and far-IR, Raman spectroscopy, and Transmission Electron Microscopy (TEM), as recently detailed [16, 19]. After laser illumination, TEM and the assimilation range in the scope of 400–800 nm were additionally acquired. The UVVis investigation was performed with a Perkin-Elmer Lambda-Bio spectrometer utilizing a 1 cm quartz cuvette to screen the size and the AuNP surface plasmon band around 520 nm.

2.4. Ingestion Cross Segment Assessment

2.4.1. Complex Dielectric Steady.

The perplexing dielectric steady $(\varepsilon_p = \varepsilon'_p + i\varepsilon''_p)$ of the AuNP was acquired from the complex refractive record of gold ($\tilde{np} = np + ikp$) at various frequencies (450 to 700 nm), as indicated by Werner et al. [20]. These qualities were adjusted by the nanoparticle size utilizing a cubic addition and determined as

$$\tilde{np} = np + ikp. \quad (1).$$

The perplexing dielectric consistent $(\varepsilon_p = \varepsilon'_p + i\varepsilon''_p)$ was acquired as follows:

$$\varepsilon_p = \left(\tilde{n_p}\right)^2 = \left(n_p + ik_p\right)^2$$
$$\varepsilon_p = \left(n_p\right)^2 - \left(k_p\right)^2 + i2\left(n_p * k_p\right), \quad (2)$$

where

$$\varepsilon'_p = \left(n_p\right)^2 - \left(k_p\right)^2$$
$$\varepsilon''_p = 2\left(n_p * k_p\right). \quad (3)$$

The complex dielectric constants were obtained for the e_m media (liver or colon tissue) following the same technique used for AuNP but using the complex index stated by Giannios et al. The experimental data were used to obtain the refractive index values as a continuous function based on the wavelength.

2.4.2. Estimations of Optical Properties of AuNP-RGD-Tissue by the Mie Hypothesis.

Hypothetical estimations were completed utilizing the summed up Mie hypothesis considering circular nanoparticles (r = 20 nm) whose measurement is lower than the light frequency (532 nm). For this situation, the Mie-Drude hypothesis was not utilized. In this way, free electron thickness was not legitimately thought of. In any case, electron development is considered by implication in the dielectric elements of materials. Mie hypothesis clarifies the cooperation between the light and

AuNPs where the ingestion and dissipating probabilities process are spoken to by the retention cross segment C_{abs} (m^2), the dispersing cross sectionC_{sca} (m^2), and the eradication cross area Cext, which is the aggregate of both (C_{ext} = C_{sca} + C_{abs}). These cross areas were determined as follows:

$$C_{ext} = \frac{24\pi^2 R^3 \varepsilon_m^{3/2}}{\lambda} * \frac{\varepsilon_p''}{\left(\varepsilon_p' + 2\varepsilon_m\right)^2 + \varepsilon_p''^2}$$

$$C_{sca} = \frac{2^7 \pi^5 R^6}{\lambda} * \left| \frac{\varepsilon_p' - \varepsilon_m}{\varepsilon_p' + 2\varepsilon_m} \right|^2 \quad (4)$$

$$C_{abs} = C_{ext} - C_{sca},$$

Where R is the particle radius and where λ is the incident WAVELLANCE. All the measurements were carried out taking into account the real and imaginary parts of AuNP dielectric constant and Fabrics.

2.5. Laser fitting.

Laser experiments were performed using a laser Nd-YAG (Qsmart-100, Quantel laser) pulsed at 5 ns at 532 nm (energy = 45.9 mJ / pulse) with 5, 10, and 15 Hz repetition frequencies. A Dual-Channel Joulemeter / Power Meter (Molectron EPM 200, Coherent) tests the power of each laser pulse. For the laser beam direction a diverging lens was used in such a way that the well plate was fully filled by the laser (diameter = 7 mm; area = 0.38 cm2) (Figure 1). During laser irradiation the well plate was mounted on a 37 C heating plate (Microplate Thermo Shaker, Human Lab MB100-2A, Hangzhou Zhejia, China).

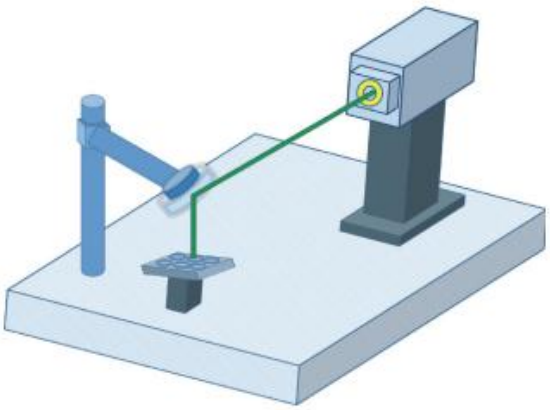

Fig.1 Laser Arrangement

3. ANALYSIS

3.1. Portrayal when Laser Light

3.1.1. Prior to Laser Light.

Spectroscopy methods and TEM pictures showed that AuNPs were functionalized with the c[RGDfK(C)] peptide in like manner with past reports [16, 19]. The normal molecule breadth was 21.56 ± 0.06 nm. The UV-Vis range demonstrated the surface plasmon reverberation band at 520 nm for AuNPs, and a red move to 522 nm for AuNP-c[RGDfK(C)] was watched. This moving is credited to the adjustments in the refraction file as a result of the connection between the peptide and the AuNP surface [16]. Raman spectroscopy and medium-and far-infrared indicated a few very much characterized groups qualities of the AuNP-c[RGDfK(C)] conjugate [16]. The Far-IR range of the AuNP-c[RGDfK(C)] indicated a trademark band at 279±1 cm−1, which is illustrative of the Au–S bond.

3.1.2. After Laser Illumination.

TEM pictures after laser illumination showed that the [RGDfK(C)] peptide remains functionalized to AuNPs surface. The molecule normal distance across changes from 21.56 ± 0.06 nm to 21.13 ± 0.07 nm (Figure 2). The watched size change after laser light on AuNP citrate-balanced out was from 20 ± 1.6 nm to 19.38 ± 0.02 nm, which can be clarified as a result of sub-atomic steric revamp on the nanoparticle surface. TEM estimations were bolstered by SPR band on UVVis spectra. The SPR for AuNP-c[RGDfK(C)] moved from 522 nm to 519.8 nm after light, while for AuNP the moving was from 520 nm to 517.5 nm (Figure 2). These movements to a lower frequency are likewise a sign of a decrease in the nanoparticle size.

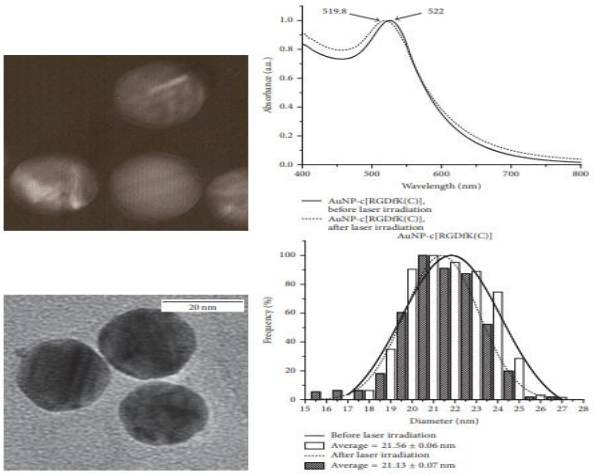

Fig.2 Morphological results before and after laser irradiation.

3.2. Assimilation Cross Area Assessment

3.2.1. Complex Dielectric Consistent.

Figure 3 shows the contrasts between the genuine and nonexistent pieces of the refractive file and dielectric steady of (a) gold, (b) liver tissue, and (c) colon tissue. The genuine piece of the dielectric consistent is identified with the put away vitality, and

the fanciful part is identified with the dissemination of the vitality inside the medium.

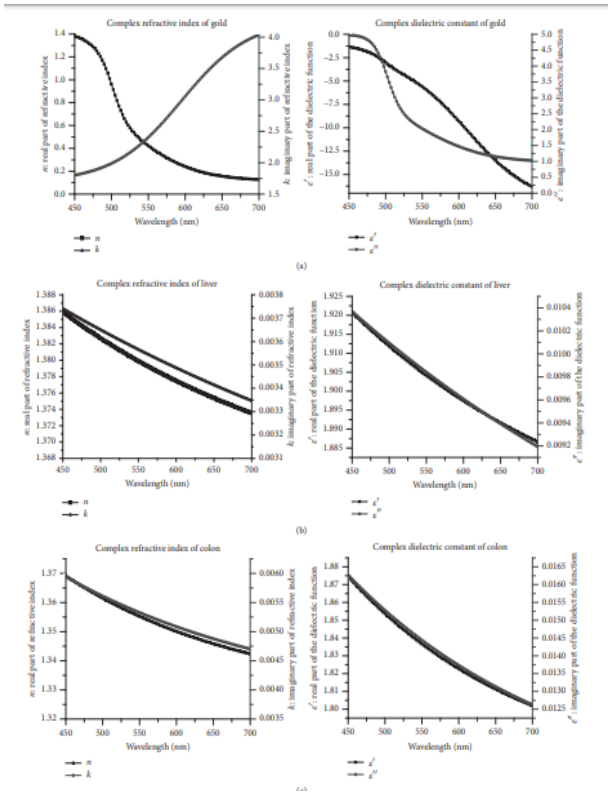

Fig.3 Real and imaginary parts of the refractive index (n, k) and dielectric constant $(\varepsilon', \varepsilon'')$ of the (a) gold, (b) liver tissue, and (c) colon tissue

3.3. Optical Coefficients of AuNP-RGD-Tissue by the Mie Hypothesis.

In concurrence with past reports [1, 4] the outcomes appeared in this exploration showed that Cext is chiefly because of the retention procedure commitment (Figure 4). The powerful retention segment speaks to the 98.96 ± 0.03% of the all out elimination compelling area (Cext).Therefore the dispersing one can be viewed as unimportant. The most extreme Cext esteem is seen at the light frequency of 522.5 nm for AuNP-RGD in a water medium and 525 nm when the nanoparticles are stored or inserted in the tissues. This outcome implies that the most extreme vitality assimilation happens at those frequencies; subsequently, the most noteworthy temperature increment rate ought to be reached at such frequencies also.

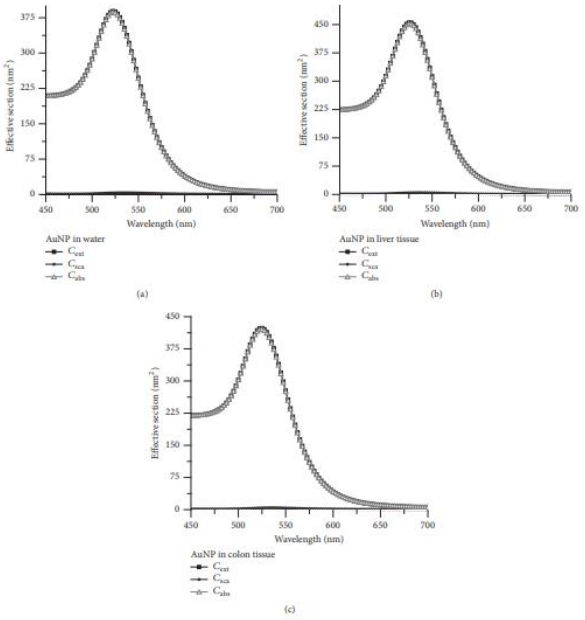

Fig.4 For AuNP in (a) water, (b) liver tissue, and (c) colon tissue, the cross section absorption, scattering and extinction.

CONCLUSION

The optical properties (assimilation and dissipating) present in gold nanoparticles (AuNPs) assume a critical job in the improvement of new photothermal removal frameworks possibly relevant in malignant growth treatment .C_{ext}, C_{abs}, and C_{sca} measurements for AuNPRGD-water, AuNP-RGD-colon, and AuNP-RGD-liver systems help to explain the temperature rise observed when irradiated at 532 nm with a Nd-YAG laser. The resulting temperature rise (about 13°C) is necessary to cause cell death by phototherapy.

REFERENCES

X. Huang and M. A. El-Sayed (2010). "Gold nanoparticles: optical properties and implementations in cancer diagnosis and photothermal therapy," Journal of Advanced Research, vol. 1, no. 1, pp. 13–28.

J. Gautier, E. Allard-Vannier, K. Herve-Aubert, M. Souc ´ e, and ´ I. Chourpa (2013). "Design strategies of hybrid metallic nanoparticles for theragnostic applications," Nanotechnology, vol. 24, no. 43, Article ID 432002.

G. Ferro-Flores, C. A. de Murphy, and L. Melendez-Alafort (2006). "Third generation radiopharmaceuticals for imaging and targeted therapy," Current Pharmaceutical Analysis, vol. 2, no. 4, pp. 339–352.

S. Hashimoto, D. Werner, and T. Uwada (2012). "Studies on the interaction of pulsed lasers

with plasmonic gold nanoparticles toward light manipulation, heat management, and nanofabrication," Journal of Photochemistry and Photobiology C: Photochemistry Reviews, vol. 13, no. 1, pp. 28–54.

R. R. Letfullin, T. F. George, G. C. Duree, and B. M. Bollinger (2008). "Ultrashort laser pulse heating of nanoparticles: Comparison of theoretical approaches," Advances in Optical Technologies, Article ID 251718.

Moores and F. Goettmann (2006). "The plasmon band in noble metal nanoparticles: an introduction to theory and applications," New Journal of Chemistry, vol. 30, no. 8, pp. 1121–1132.

R. R. Letfullin, C. B. Iversen, and T. F. George (2011). "Modeling nanophotothermal therapy: Kinetics of thermal ablation of healthy and cancerous cell organelles and gold nanoparticles," Nanomedicine: Nanotechnology, Biology and Medicine, vol. 7, no. 2, pp. 137–145.

H. Mendoza-Nava, G. Ferro-Flores, B. Ocampo-Garc´ıa et. al. (2013). "Laser heating of gold nanospheres functionalized with octreotide: in vitro effect on hela cell viability," Photomedicine and Laser Surgery, vol. 31, no. 1, pp. 17–22.

N. N. Nedyalkov, S. E. Imamova, P. A. Atanasov et. al. (2011). "Interaction of gold nanoparticles with nanosecond laser pulses: Nanoparticle heating," Applied Surface Science, vol. 257, no. 12, pp. 5456–5459.

L. Sanchez-Hern ´ andez, G. Ferro-Flores, N. P. Jim ´enez-Mancilla ´ et. al. (2015). "Comparative effect between laser and radiofrequency heating of rgd-gold nanospheres on MCF7 cell viability," Journal of Nanoscience and Nanotechnology, vol. 15, no. 12, pp. 9840–9848.

X. Huang, P. K. Jain, I. H. El-Sayed, and M. A. El-Sayed (2008). "Plasmonic photothermal therapy (PPTT) using gold nanoparticles," Lasers in Medical Science, vol. 23, no. 3, pp. 217–228.

M. X. Wang, J. D. Brodin, J. A. Millan et. al. (2017). "Altering DNAprogrammable colloidal crystallization paths by modulating particle repulsion," Nano Letters, vol. 17, no. 8, pp. 5126–5132.

P. K. Jain, K. S. Lee, I. H. El-Sayed, and M. A. El-Sayed (2006). "Calculated absorption and scattering properties of gold nanoparticles of different size, shape, and composition: applications in biological imaging and biomedicine," The Journal of Physical Chemistry B, vol. 110, no. 14, pp. 7238–7248.

G. Ferro-Flores, B. E. Ocampo-Garc´ıa, C. L. Santos-Cuevas, E. Morales-Avila, and E. Azor´ın-Vega (2014). "Multifunctional radiolabeled nanoparticles for targeted therapy," Current Medicinal Chemistry, vol. 21, no. 1, pp. 124–138.

Cantelli, G. Battistelli, G. Guidetti, J. Manzi, M. Di Giosia, and M. Montalti (2016). "Luminescent gold nanoclusters as biocompatible probes for optical imaging and theranostics," Dyes and Pigments, vol. 135, pp. 64–79.

M. Luna-Gutierrez, G. Ferro-Flores, B. Ocampo-Garc´´ıa et. al. (2012). "177Lu-labeled monomeric, dimeric and multimeric RGD peptides for the therapy of tumors expressing (])β(3) integrins," Journal of Labelled Compounds and Radiopharmaceuticals, vol. 55, no. 4, pp. 140–148.

Corresponding Author

Komal*

PhD Scholar, OPJS University, Churu, Rajasthan